Overlapping functions between XLF repair protein and 53BP1 DNA damage response factor in end joining and lymphocyte development

Xiangyu Liu[a,1], Wenxia Jiang[a,1], Richard L. Dubois[a], Kenta Yamamoto[a,b], Zachary Wolner[a], and Shan Zha[a,2]

[a]Department of Pathology and Cell Biology and Department of Pediatrics, Institute for Cancer Genetics, College of Physicians and Surgeons, Columbia University, New York, NY 10032; and [b]Graduate program of Pathobiology and Molecular Medicine, College of Physicians and Surgeons, Columbia University, New York, NY 10032

Edited* by Michel C. Nussenzweig, The Rockefeller University, New York, NY, and approved January 31, 2012 (received for review December 8, 2011)

Nonhomologous end joining (NHEJ), a major pathway of DNA double-strand break (DSB) repair, is required during lymphocyte development to resolve the programmed DSBs generated during Variable, Diverse, and Joining [V(D)J] recombination. XRCC4-like factor (XLF) (also called Cernunnos or NHEJ1) is a unique component of the NHEJ pathway. Although germ-line mutations of other NHEJ factors abrogate lymphocyte development and lead to severe combined immunodeficiency (SCID), XLF mutations cause a progressive lymphocytopenia that is generally less severe than SCID. Accordingly, XLF-deficient murine lymphocytes show no measurable defects in V(D)J recombination. We reported earlier that ATM kinase and its substrate histone H2AX are both essential for V(D)J recombination in XLF-deficient lymphocytes, despite moderate role in V(D)J recombination in WT cells. p53-binding protein 1 (53BP1) is another substrate of ATM. 53BP1 deficiency led to small reduction of peripheral lymphocyte number by compromising both synapse and end-joining at modest level during V(D)J recombination. Here, we report that 53BP1/XLF double deficiency blocks lymphocyte development at early progenitor stages, owing to severe defects in end joining during chromosomal V(D)J recombination. The unrepaired DNA ends are rapidly degraded in 53BP1$^{-/-}$XLF$^{-/-}$ cells, as reported for H2AX$^{-/-}$XLF$^{-/-}$ cells, revealing an end protection role for 53BP1 reminiscent of H2AX. In contrast to the early embryonic lethality of H2AX$^{-/-}$XLF$^{-/-}$ mice, 53BP1$^{-/-}$XLF$^{-/-}$ mice are born alive and develop thymic lymphomas with translocations involving the T-cell receptor loci. Together, our findings identify a unique function for 53BP1 in end-joining and tumor suppression.

Ataxia-Telangiectasia-Mutated | XRCC4-like factor | classical nonhomologous end joining

Lymphocyte development requires the ordered assembly of variable region of antigen receptor genes from individual Variable, Diverse, and Joining gene segments through V(D)J recombination (1). V(D)J recombination is initiated by the RAG endonuclease (RAG), which introduces DNA double-strand breaks (DSBs) between the conserved recombination signal sequence (RSS) and the participating germ-line V, D, or J gene segments (1). RAG cleavage generates two types of DNA ends, the 5′-phosphorylated blunt signal ends (SEs) and the hairpin sealed coding ends (CEs) (1). In the next step, ubiquitously expressed classical nonhomologous end-joining (C-NHEJ) factors directly join the two SEs to form a signal join (SJ), and process (via hairpin opening, de novo synthesis, and loss of nucleotides) and join the two CEs to form a coding join (CJ) (1).

There are seven C-NHEJ factors in mammalian cells. Ku70 and Ku80 (or KU86 in human) form heterodimers (KU) that bind DSB ends and, among other functions, recruit and activate other NHEJ factors (2). DNA-bound KU interacts with the DNA-PK catalytic subunit (DNA-PKcs), and together they activate the endonuclease function of Artemis for end processing, including opening hairpin-sealed CEs during V(D)J recombination (2). Finally, the complex formed by Ligase 4, XRCC4 and likely XRCC4-like factor (XLF) (also called Cernunnos or NHEJ1) ligates the ends together. XLF binds XRCC4 and shares structural similarity with XRCC4 (3–6). However, the exact role of XLF in C-NHEJ is not completely understood.

C-NHEJ is essential for V(D)J recombination. Accordingly, defects in all previously characterized NHEJ factors (except XLF, see below) completely block lymphocyte development at the progenitor stage and cause T$^-$ and B$^-$ severe combined immunodeficiency (T$^-$B$^-$SCID) in both human patients and mouse models (1, 2, 7). In p53-deficient backgrounds, the unrepaired programmed DSBs in C-NHEJ–deficient mice participate oncogenic chromosomal translocations and eventually lead to lymphomas (1). XLF mutations cause a progressive lymphocytopenia that is usually less severe than SCID (3, 4, 8) in human patients. XLF-deficient mice have reduced lymphocyte numbers, but do not exhibit stage-specific blockade (7). Consistently, XLF-deficient lymphocytes perform chromosomal V(D)J recombination normally, despite severe defects in extrachromosomal V(D)J recombination in XLF-deficient murine embryonic stem cells (7, 9), suggesting one or several other repair pathway(s) might exist in developing lymphocytes to compensate for the loss of XLF during V(D)J recombination. Recently we reported that chromosomal V(D)J recombination in XLF-deficient lymphocytes require ATM and its kinase activity (10).

ATM kinase is a master regulator of the DNA damage response. Upon formation of DSBs, including those occurring during normal V(D)J recombination, ATM is activated and phosphorylates its substrates (e.g., histone H2AX, 53BP1) involved in DNA repair and cell cycle checkpoints (11, 12). Although ATM promotes efficient and accurate DNA repair during CJ formation (13), ATM and its substrates are not strictly required for V(D)J recombination and lymphocyte development (14, 15). Therefore, it is surprising that ATM/XLF double deficiency completely abrogates lymphocyte development at the early progenitor stages, similar to previously characterized C-NHEJ deficiencies (1, 10). When stimulated to perform V(D)J recombination, ATM$^{-/-}$XLF$^{-/-}$ B cells fail to generate rearrangement products (CJs and SJs), but instead accumulate unrepaired CEs and SEs—indicating severe end-joining defects (10). The function of ATM in V(D)J recombination of XLF-deficient lymphocytes requires ATM kinase activity and, at least in part, its substrate histone H2AX (10). Surprisingly, although ATM$^{-/-}$XLF$^{-/-}$ mice are born alive, H2AX$^{-/-}$XLF$^{-/-}$ mice are embryonic lethal (10). At the molecular level, the unrepaired CEs/SEs generated during V(D)J recombination are readily detectable in ATM$^{-/-}$XLF$^{-/-}$ cells, but degraded in H2AX$^{-/-}$XLF$^{-/-}$ cells

Author contributions: X.L., W.J., K.Y., and S.Z. designed research; X.L., W.J., R.L.D., K.Y., Z.W., and S.Z. performed research; S.Z. contributed new reagents/analytic tools; X.L., W.J., R.L.D., K.Y., and S.Z. analyzed data; and X.L., W.J., and S.Z. wrote the paper.

The authors declare no conflict of interest.

*This Direct Submission article had a prearranged editor.

[1]X.L. and W.J. contributed equally to this work.

[2]To whom correspondence should be addressed. E-mail: sz2296@columbia.edu.

This article contains supporting information online at www.pnas.org/lookup/suppl/doi:10.1073/pnas.1120160109/-/DCSupplemental.

IMMUNOLOGY

(10). Although a recent study revealed that phosphorylated-H2AX (γ-H2AX) protects unrepaired CEs/SEs from ATM- and CtIP-mediated resection (16), it is not known whether excessive end resection causes the embryonic lethality of H2AX$^{-/-}$XLF$^{-/-}$ mice. Likewise, the mechanisms by which ATM, H2AX, and potentially other ATM substrates promote end-joining in XLF-deficient cells remain unknown. In addition to XLF, ATM also has redundant function with DNA-PKcs, another member of the NHEJ pathway in the SJ formation during V(D)J recombination (17, 18) and in DSB repair during mature B cells class switch recombination (19).

53BP1 is another substrate of ATM that has been implicated in DSB repair and lymphocyte development (20, 21). Although 53BP1 could form transient foci in H2AX-deficient cells (22), the normal recruitment of 53BP1 to DSBs requires γ-H2AX, MDC1, and two E3 ligases—RNF8 and RNF168 (23). The retention of 53BP1 at DSBs is mediated by its tandem Tudor domains, which bind to methylated targets including histones (24). The C terminus of 53BP1 harbors two tandem BRCT domains, which, among other functions, bind the p53 tumor suppressor (25). A recent study found that the Tudor domains, but not the BRCT domains, of 53BP1 are required for immunoglobulin(Ig) class switch recombination (CSR) (26). The same study also identified a role for 53BP1 in end protection during CSR and the repair of I-SceI endonuclease-generated DSBs (26). Similar to H2AX, 53BP1 is not required for V(D)J recombination or lymphocyte development. 53BP1 deficiency reduces peripheral lymphocyte number with, at most, a very mild effect of chromosomal V(D)J recombination. Although the role for 53BP1 in promoting synapsis between distal V and J segments might explain the reduced lymphocyte number (20, 21, 26), a critical role of 53BP1 in end joining during lymphocyte development has not been characterized.

Here, we have generated and characterized 53BP1 and XLF double-deficient mice. Our results reveal a critical function for 53BP1 in end-joining and end protection during V(D)J recombination and uncover a unique role for 53BP1 in tumor suppression.

Results

Lymphocyte Development Is Blocked at Early Progenitor Stages in 53BP1/XLF Double-Deficient Mice. To test whether 53BP1 has overlapping functions with XLF in DNA repair, we generated 53BP1/XLF double-deficient animals by intercrossing 53BP1$^{-/-}$XLF$^{+/-}$ mice. Notably, 12 of the 43 progenies analyzed (27.9%) from five independent breeding pairs were 53BP1$^{-/-}$XLF$^{-/-}$, similar to the expected frequency of 25% (Fig. S1*A*), indicating that 53BP1/XLF double deficiency does not block embryonic development. This result is intriguing given that H2AX$^{-/-}$XLF$^{-/-}$ mice are embryonic lethal (10). At 3 wk of age, 53BP1$^{-/-}$XLF$^{-/-}$ mice, like ATM$^{-/-}$XLF$^{-/-}$ mice, are ≈50% smaller than age- and sex-matched WT, 53BP1$^{-/-}$, or XLF$^{-/-}$ mice (Fig. S1*B*) (10), indicating that 53BP1 and XLF have overlapping functions in general cell proliferation.

Total thymocyte number was reduced ≈20-fold in 4- to 8-wk-old 53BP1$^{-/-}$XLF$^{-/-}$ mice in comparison with XLF$^{-/-}$ or 53BP1$^{-/-}$ mice, which only exhibit a mild reduction in lymphocyte numbers (approximately two- to threefold reduction of thymocytes) (Fig. S2*A*). The severe reduction of thymocyte number in 53BP1$^{-/-}$XLF$^{-/-}$ mice is similar to that observed in C-NHEJ–deficient animals (e.g., DNA-PKcs$^{-/-}$) (1) (Fig. S2*A*). Flow cytometric analysis revealed that T-cell development in 53BP1$^{-/-}$XLF$^{-/-}$ mice is blocked at the CD4^{-}CD8^{-} double negative (DN) stage (Fig. 1*A*), particularly at the DN II (CD44^{+}CD25^{+}) and DN III (CD44^{-}CD25^{+}) stages when T-cell receptor (TCR)β/δ/γ loci are undergoing V(D)J recombination (Fig. 1*A*). This phenotype is very similar to C-NHEJ–deficient mice with leaky SCID (such as the DNA-PKcs$^{-/-}$ mouse shown in Fig. 1*A*). The few 53BP1$^{-/-}$XLF$^{-/-}$ T cells that mature into CD4^{+}CD8^{+} double-positive (DP) thymocytes are again blocked at TCRα rearrangement, as evidenced by the reduced surface CD3ε/TCRβ expression within the DP population and the greatly reduced numbers of CD4^{+}CD8^{-} or CD4^{-}CD8^{+} single-positive (SP) T cells (Fig. 1*A*). B-cell development in the bone marrow of 53BP1$^{-/-}$XLF$^{-/-}$ mice is also severely blocked at the progenitor-B (Pro-B, B220^{+}CD43^{+}IgM^{-}) cell stage, when V(D)J recombination at the Ig heavy chain (IgH) locus is initiated (Fig. 1*B*). Very few pre-B cells (B220^{+}CD43^{-}IgM^{-}) and almost no mature B cells (B220^{+}CD43^{-}IgM^{+}) could be found in the bone marrow of 53BP1$^{-/-}$XLF$^{-/-}$ mice. Correspondingly, peripheral B-cell number is reduced more than threefold in the spleen and lymph nodes of 53BP1$^{-/-}$XLF$^{-/-}$ mice (Figs. 1*B* and 2 and Fig. S2*A*).

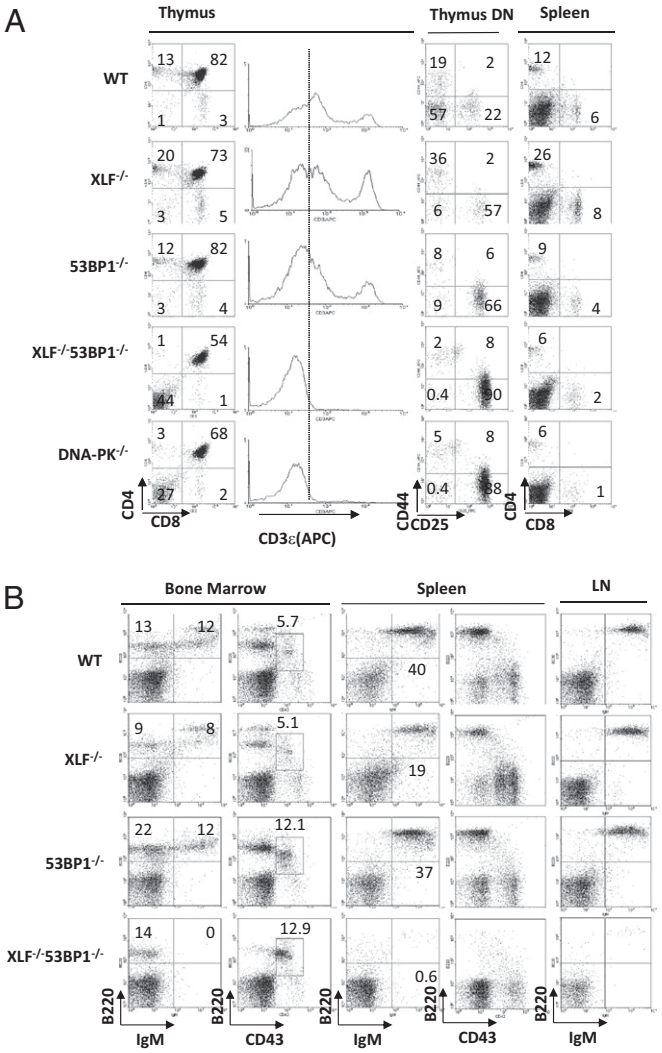

Fig. 1. XLF and 53BP1 have redundant functions in lymphocyte development. (*A*) Representative flow cytometric analyses of T cells in thymus and spleen from WT, XLF$^{-/-}$, 53BP1$^{-/-}$, 53BP1$^{-/-}$XLF$^{-/-}$, and DNA-PKcs$^{-/-}$ mice (see *Experimental Procedures* for further description of the mouse lines). The histogram represents the total live thymocytes. The dashed line in the histogram provides a visual reference for the relative level of surface CD3ε staining. DN, CD4^{-}CD8^{-} double negative. For the "Thymus DN" staining, the total population is thymic DN cells, not total thymocytes. (*B*) Representative flow cytometric analyses of B cells in bone marrow, spleen, and lymph node from WT, XLF$^{-/-}$, 53BP1$^{-/-}$, and 53BP1$^{-/-}$XLF$^{-/-}$ mice. The numbers on each blot (*A* and *B*) represent the percentage of live cells represented by a given population.

Impaired V(D)J Recombination Underlies the Lymphocyte Development Defects of 53BP1$^{-/-}$XLF$^{-/-}$ Mice. Lymphocyte development requires bursts of cell proliferation after each round of V(D)J recombination. Therefore, mutations in proteins required for proliferation or survival (e.g., BRCA1 or DICER) block lymphocyte development without specifically affecting V(D)J

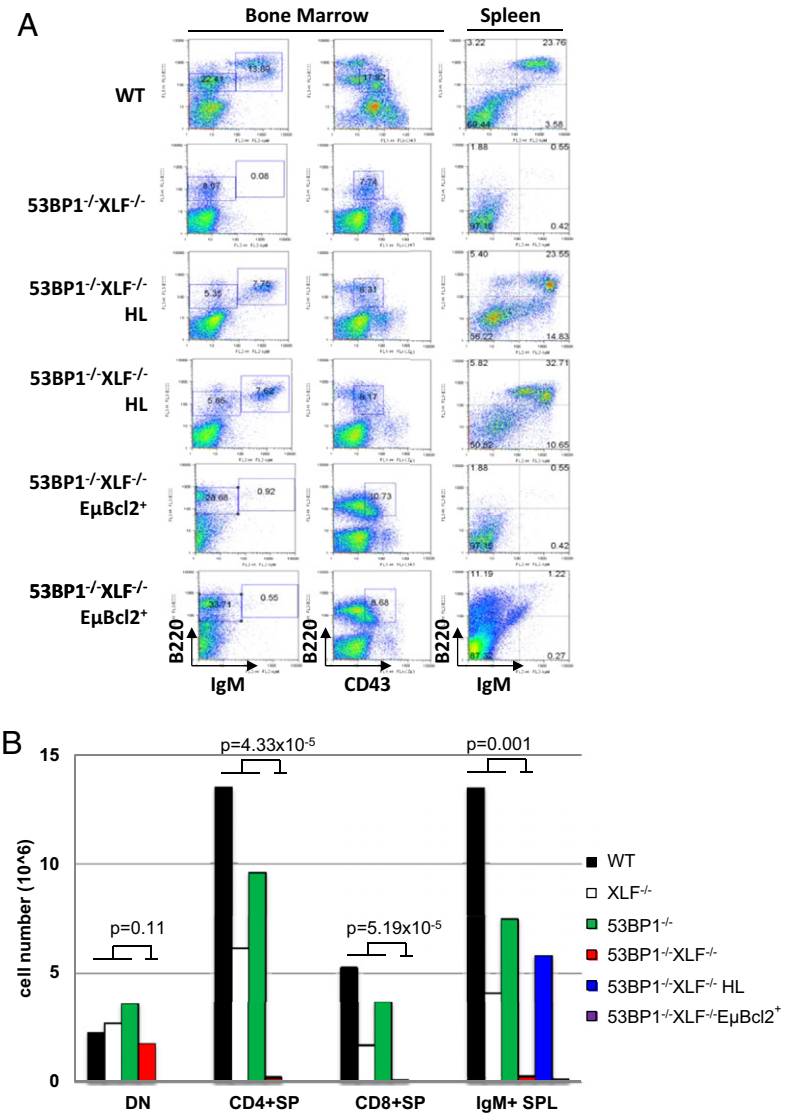

Fig. 2. Lymphocyte development defects in 53BP1$^{-/-}$XLF$^{-/-}$ mice are due to impaired V(D)J recombination. (*A*) Representative flow cytometric analyses of bone marrow and spleen from WT, XLF$^{-/-}$53BP1$^{-/-}$, 53BP1$^{-/-}$XLF$^{-/-}$HL, and 53BP1$^{-/-}$XLF$^{-/-}$EμBcl2+ mice. Numbers on the plot are percentage of total live cells (determined by forward and side scatter) represented by indicated population. (*B*) The number of total DN and single-positive (SP) thymocytes and IgM^{+} splenic B cells were calculated based on total organ cellularity and the percentage of the given cell type (by flow cytometric analyses). Each value listed represents the average ± SD from at least three mice of each genotype between 4 and 12 wk of age. The *P* values are calculated between corresponding groups by using two-tailed Student's *t* test. The original data are provided in Fig. S2.

recombination (27, 28). To distinguish whether the developmental abnormalities of 53BP1$^{-/-}$XLF$^{-/-}$ lymphocytes are caused by defects in V(D)J recombination or cell proliferation/survival, we generated 53BP1$^{-/-}$XLF$^{-/-}$ mice with either preassembled IgH and Igκ genes (referred to as "HL mice") (29, 30) or the EμBcl-2 transgene (31). We found that the EμBcl-2 transgene increased the size of pro–B-cell population in 53BP1$^{-/-}$XLF$^{-/-}$ mice, but failed to rescue B-cell development or peripheral B-cell number (Fig. 2 *A* and *B* and Fig. S2*B*). Meanwhile, HL knockin bypasses the requirement for V(D)J recombination during B-cell development, and significantly rescued B-cell development and restored peripheral B-cell numbers in 53BP1$^{-/-}$XLF$^{-/-}$ HL mice (Fig. 2 *A* and *B* and Fig. S2*B*). Together these findings suggest that 53BP1/XLF double deficiency blocks lymphocyte development by impairing V(D)J recombination.

53BP1$^{-/-}$XLF$^{-/-}$ Cells Have End-Joining Defects During V(D)J Recombination. To further characterize the V(D)J recombination defects, we generated v-abl kinase transformed immature B-cell lines from the bone marrows of WT, XLF$^{-/-}$, 53BP1$^{-/-}$, and 53BP1$^{-/-}$XLF$^{-/-}$ mice carrying the EμBcl-2 transgene (7, 13). In the WT cells, treatment with STI571 (Gleevec; Imatinib), an inhibitor of the *v-abl* kinase, induces G_1 cell cycle arrest, RAG expression, and efficient V(D)J recombination of integrated V(D)J recombination substrates. pMX-INV is an inversional retrovirus V(D)J recombination substrate that can activate GFP expression upon successful V(D)J recombination (7, 13) (Fig. 3*A*). We generated two or more independent *v-abl* transformed B-cell lines from each genotype and introduced the pMX-INV substrate into them. To examine V(D)J recombination, GFP expression was measured by flow cytometry at 0 (control), 2, or 4 d after treatment with STI571, and the rearrangement status and recombination intermediates were visualized by Southern blot analysis. A significant fraction of WT and XLF$^{-/-}$ B cells successfully rearranged the inversional V(D)J recombination substrate as indicated by robust GFP expression and the appearance of the CJ products in Southern blot (Fig. 3*B* and Fig. S3). As previously reported, an ATM kinase inhibitor blocks V(D)J recombination in XLF$^{-/-}$ cells (10), leading to an accumulation of CEs instead of CJ products (Fig. 3*B* and Fig. S3). We found that 53BP1$^{-/-}$ cells perform robust V(D)J recombination (Fig. 3*B* and Fig. S3), consistent with largely normal lymphocyte development in 53BP1$^{-/-}$ mice (20, 32). In contrast, multiple 53BP1$^{-/-}$XLF$^{-/-}$ cell lines showed greatly reduced GFP expression (Figs. S3 and S4 and Fig. 4*A*) and the absence of rearrangement products (CJ) (Figs. 3 *B* and *C* and 4*B*) after STI571 treatment. Moreover, unlike ATM kinase inhibitor treated XLF$^{-/-}$ cells, very little, if any, CEs accumulated in 53BP1$^{-/-}$XLF$^{-/-}$ cells (Figs. 3 *B* and *C* and 4*B*).

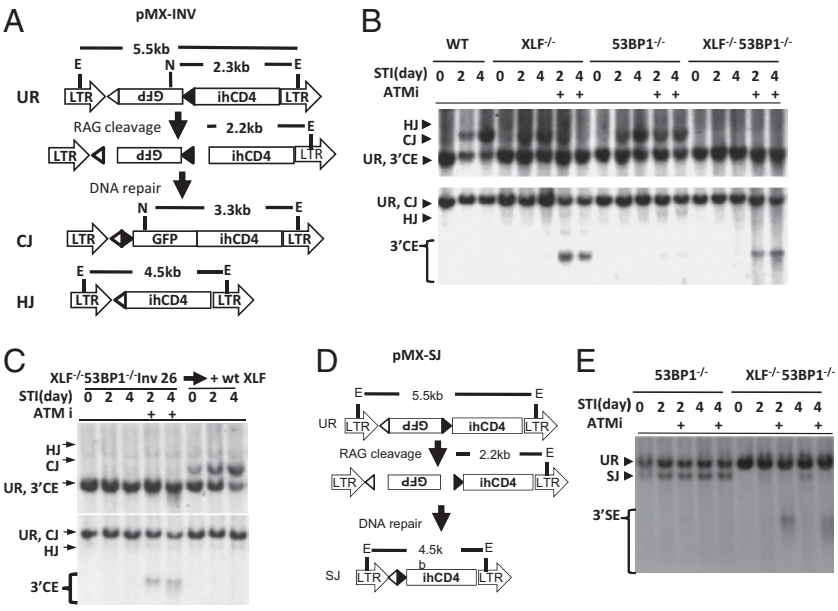

Fig. 3. 53BP1$^{-/-}$XLF$^{-/-}$ B cells have end joining during chromosomal V(D)J recombination. (*A* and *D*) Schematic of the pMX-INV (*A*) and pMX -SJ (*B*) retroviral V(D)J recombination substrates (13). The diagrams illustrate the unrearranged substrate (UR), CE/SE intermediates, and CJ/SJ products. The RSS (open and filled triangles), GFP, IRES-truncated hCD4 (ihCD4), and the LTRs are marked. The positions of EcoRV (E) sites and NcoI (N) sites are shown. hCD4 probe is located within ihCD4. (*B* and *C*) Southern blot analysis with hCD4 probe of EcoRV+NcoI (*Upper*) and EcoRV (*Lower*) digested genomic DNA from the indicated *v-abl*–transformed B cells containing pMX-INV substrates treated with STI571 for 2 or 4 d with or without ATM kinase inhibitor (15 μM). (*E*) Southern blot analysis with hCD4 probe of EcoRV digested genomic DNA from the indicated lines containing integrated pMX-SJ substrate The results shown in *B* and *E* were obtained from pools of B-cell lines with diverse integration sites of given substrate. *C* showed the result of cell line with single clonal integration of pMX-INV and the corresponding clones with ectopic expression of XLF.

Lack of CJ in the absence of CE accumulation could be caused by either reduced RAG cleavage or by aberrant end resection coupled with end joining defects. We previously showed that the simultaneous lack of CEs and CJs in H2AX$^{-/-}$XLF$^{-/-}$ cells occurs because γ-H2AX is required to protect unrepaired CEs from ATM-mediated degradation (10). To test whether 53BP1 has a similar function as H2AX in end protection, we performed V(D)J recombination assays in 53BP1$^{-/-}$XLF$^{-/-}$ cells treated with ATM kinase inhibitor (Fig. 3 *B* and *C*). In STI571-treated 53BP1$^{-/-}$XLF$^{-/-}$ cells, ATM kinase inhibitor led to the appearance of a visible CE band with CE smear, a characteristic feature of end degradation (Figs. 3 *B* and *C* and 4*B*). Notably, ATM inhibition slightly, but consistently, reduced GFP expression in 53BP1$^{-/-}$XLF$^{-/-}$ cells, suggesting that ATM has a 53BP1-independent function in end joining in XLF$^{-/-}$ cells (Figs. 3 *B* and *C* and 4*B* and Fig. S3).

To evaluate whether a defect in RAG cleavage contributes to the absence of CJ formation in 53BP1$^{-/-}$XLF$^{-/-}$ cells, XLF expression was reconstituted in XLF$^{-/-}$ and 53BP1$^{-/-}$XLF$^{-/-}$ cells that harbor a single clonally integrated V(D)J recombination substrate. XLF reconstitution was achieved by infection with an XLF-encoding retrovirus that carries an IRES-human CD2 (hCD2) marker for purification (Fig. S4*A*), and XLF expression was verified by Western blot analysis (Fig. S4*B*). Significantly, ectopic XLF restored V(D)J recombination in multiple 53BP1$^{-/-}$XLF$^{-/-}$ cell lines bearing unique substrate integration sites (inv26 and inv21), and in XLF$^{-/-}$ cells treated with ATM kinase inhibitor (Fig. 3*C* and Fig. S4 *C*–*E*), implying robust RAG cleavage in these lines. Moreover, Southern blot analyses confirmed the formation of correct rearrangement products and the absence of CEs in XLF-reconstituted 53BP1$^{-/-}$XLF$^{-/-}$ cells (Fig. 3*C*).

Finally, to identify resected DNA ends in 53BP1$^{-/-}$XLF$^{-/-}$ cells directly, we carried out 3D-interphase FISH analyses on G_1-arrested STI571-treated cells. For this assay, we mapped the substrate integration site in 53BP1$^{-/-}$XLF$^{-/-}$Inv21 and control XLF$^{-/-}$Inv122 cells and developed FISH probes that cover the substrate integration site and the flanking region (≈100 kb on both sides) (Fig. S5*A*). Whereas two dots in a nucleus represent the two homologous chromosomes, three dots would presumably arise by chromosomal breakage within the integrated V(D)J recombination substrate (Fig. S5 *A* and *B*). As proof of principle, ATM inhibition increased the frequency of three-dot nuclei from 2.5 to 10.5% in STI571-treated XLF$^{-/-}$Inv122 cells (P = 0.001) (Figs. S5*C* and 6). Consistent with end-joining defects in 53BP1$^{-/-}$XLF$^{-/-}$ cells, the frequency of three-dot nuclei was reduced from 11.1 to 7.0% upon ectopic XLF reconstitution of STI571-treated 53BP1$^{-/-}$XLF$^{-/-}$Inv21 cells (P = 0.01) (Figs. S5*D* and 6). Among other possibilities, the low residual level of three-dot nuclei observed in STI treated 53BP1$^{-/-}$XLF$^{-/-}$Inv21 cells + XLF cells may be caused by a low level of residual DNA replication under STI571 treated conditions (13).

Successful rearrangement of inversional V(D)J recombination substrate requires hairpin opening at the CEs and formation of both CJs and SJs. To ascertain whether CJ and SJ formation are both affected in 53BP1$^{-/-}$XLF$^{-/-}$ cells, we introduced deletional V(D)J recombination substrates designed to test CJ (pMX-CJ; Fig. S7*A*) and SJ (pMX-SJ, Fig. 3*D*) formation separately into *v-abl*–transformed B cells of different genotypes. Although WT, 53BP1$^{-/-}$, or XLF$^{-/-}$ cells generated CJs and SJs efficiently without accumulation of CEs or SEs (Fig. 3*E* and Fig. S7*B*), 53BP1$^{-/-}$XLF$^{-/-}$ cells displayed severe impairment of both CJ and SJ formation and significant accumulation of CEs or SEs upon ATM inhibition (Fig. 3*E* and Fig. S7*B*), indicating that 53BP1$^{-/-}$XLF$^{-/-}$ cells have defects in end-joining during both CJ and SJ formation. Consistent with the redundant function between 53BP1 and XLF in end joining in general, 53BP1$^{-/-}$XLF$^{-/-}$ cells are hypersensitive to ionizing radiation to a level similar to XRCC4-deficient cells (Fig. S7*C*). Finally, urea denaturing gel analysis showed that the CEs that accumulate in 53BP1$^{-/-}$XLF$^{-/-}$ cells have the open-hairpin configuration (Fig. S8). Together, these findings indicate that 53BP1, like H2AX, promotes end joining and protects the unrepaired DNA ends from ATM-dependent resection.

Tudor Domains, but Not the BRCT Domains, of 53BP1 Are Required for End Joining in XLF$^{-/-}$ Cells. 53BP1 has two prominent domains that have been implicated in DNA repair—the Tudor domains and the C-terminal BRCT domains. To determine which of these are required for V(D)J recombination in XLF-deficient cells, we used retroviral expression vectors to reconstitute 53BP1$^{-/-}$XLF$^{-/-}$Inv26 cells with either WT mouse 53BP1 or 53BP1 derivatives that bear a missense mutation (D1518R) disrupting the Tudor domains (53BP1^{Tudor}) or a truncation removing the tandem BRCT domains (53BP1$^{\Delta BRCT}$) (Fig. S4*A*). Although the large size of the 53BP1 coding sequence (5,910 base pairs in ORF) significantly affects retroviral packaging, we were able to express full-length mouse 53BP1 in 53BP1$^{-/-}$XLF$^{-/-}$Inv26 cells after purification based on hCD2^{+} expression (Fig. S9*A*). As expected, reconstitution of STI571-treated 53BP1$^{-/-}$XLF$^{-/-}$ Inv26 cells with ectopic WT 53BP1 increased the proportion of

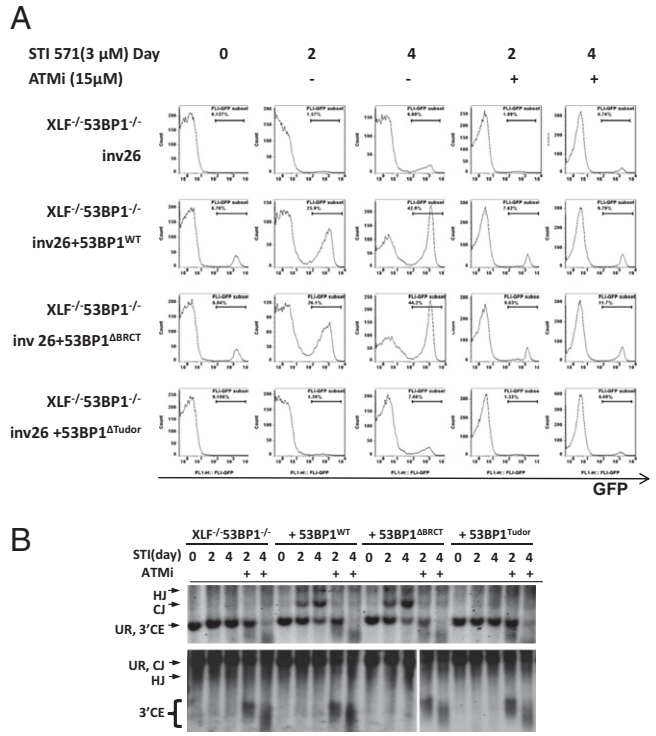

Fig. 4. End-joining in XLF$^{-/-}$ B cells requires the Tudor domain, but not the BRCT domain, of 53BP1. 53BP1$^{-/-}$XLF$^{-/-}$ B cells with single clonal integration of pMX-INV (Inv 26) cells were infected with pBMN-ihCD2-53BP1^{WT}, pBMN-ihCD2-53BP1$^{\Delta BRCT}$, or pBMN-ihCD2-53BP1$^{\Delta BRCT}$. (*A*) Flow cytometry analysis for GFP expression in different cells with identical substrate integration treated with STI for 0, 2, or 4 d with or without ATM inhibitor. (*B*) Southern blot analysis with hCD4 probe of EcoRV+NcoI (*Upper*) and EcoRV (*Lower*) digested genomic DNA from the indicated *v-abl*–transformed B cells treated with STI571 with or without ATM inhibitor as indicated.

the GFP+ cells from ≈6% to nearly 40% (Fig. 4*A*) and the corresponding CJs detectable by Southern blot analysis (Fig. 4*B*). Notably, V(D)J recombination in 53BP1$^{-/-}$XLF$^{-/-}$Inv26 reconstituted with ectopic 53BP1 still required ATM kinase activity, because they are still XLF-deficient. Interestingly, ectopic expression of 53BP1$^{\Delta BRCT}$ restored V(D)J recombination and CJ/SJ formation to levels comparable to those attained by reconstitution with WT 53BP1. In contrast, 53BP1^{Tudor} failed to restore V(D)J recombination or protect unrepaired ends from degradation (Fig. 4 *A* and *B*). These results indicate that the Tudor domains, but not the BRCT repeats, of 53BP1 are required for both end joining and end protection during V(D)J recombination.

53BP1 and XLF Double-Deficient Mice Developed Thymic Lymphomas with Chromosomal Translocations Involving the TCR Loci. Although thymic lymphomas are rarely observed in mice deficient for 53BP1 or XLF alone, three of four 53BP1$^{-/-}$XLF$^{-/-}$ mice developed thymic lymphomas at 4 mo of age (average survival = 123 d) (Fig. S10*A*). Flow cytometry analysis revealed that the 53BP1$^{-/-}$XLF$^{-/-}$ tumors are comprised of immature CD3^{low}DP or CD3^{low}CD8^{+} cells (Fig. S10*B*) that displayed clonal TCRβ rearrangements upon Southern blot analysis (Fig. S10*C*). In one of the tumors, chromosome paint and TCRα locus specific FISH analyses revealed a clonal translocation between chromosome 12 and chromosome 14 involving the TCRα/δ locus (Fig. S10*D*). Together, these findings imply that XLF and 53BP1 have overlapping functions in both DNA repair and tumor suppression.

Discussion

53BP1 is phosphorylated by ATM and forms nuclear foci that colocalize with γ-H2AX at sites of DSBs (23). Using *v-abl* transformed B cells, we now show that 53BP1 deficiency does not detectably affect chromosomal V(D)J recombination. However, 53BP1 is required for end ligation during chromosomal V(D)J recombination in XLF-deficient lymphocytes, similar to ATM and H2AX (Figs. 1–3) (10). Given that H2AX is required for DSB-induced focus formation of many proteins, this result suggests that other proteins not required for 53BP1 foci formation (e.g., BRCA1, RAD50) are likely dispensable for end joining in XLF-deficient cells. In addition, we observe that 53BP1 protected unrepaired ends from degradation (Fig. 3) in a manner reminiscent of H2AX (10). In this context, the end protection role of 53BP1 described here is similar to that reported for 53BP1 during CSR and during repair of I-SceI endonuclease-generated DSBs (21, 26). Unlike the proliferating cells used to study CSR or I-SceI-induced DSB repair, the unrepaired CEs/SEs we observe in *v-abl*–transformed B cells accumulate in strictly G_1-arrested cells, indicating that the end protection role of 53BP1 is not limited to cells programmed to use end resection as the first step for homology-directed repair. In addition, we have found that the end joining and end protection functions of 53BP1 require its Tudor domains and, by extension, the ability of 53BP1 to bind methylated targets, but does not require the C-terminal BRCT domains (Fig. 4). Finally, our study also revealed that, in addition to end joining, 53BP1 and XLF have overlapping functions in tumor suppression (Fig. S10).

During the DNA damage response, ATM phosphorylates H2AX to generate γ-H2AX at the chromatin adjacent to DSBs. Phosphorylated H2AX recruits MDC1 and two E3 ubiquitin ligases—RNF8 and RNF168 (23) to DSB chromatin, and these factors, in turn, recruit 53BP1 through a mechanism that might involve histone methyl-transferase MMSET (33). The end-ligation and end-protection defects of 53BP1$^{-/-}$XLF$^{-/-}$ B cells are very similar to those reported for H2AX$^{-/-}$XLF$^{-/-}$ cells. Therefore, it is tempting to speculate that MDC1, RNF8, RNF168, or even MMSET might be similarly required for V(D)J recombination, end ligation, and end protection in XLF-deficient cells. Among other possibilities, H2AX and 53BP1 might protect the unrepaired DNA ends by forming physically prevent the end-processing enzyme. Alternatively H2AX, 53BP1, and other chromatin factors might modify the chromatin stage to prevent extensive nucleosome unpacking. ATM inhibition modestly, but consistently, reduced V(D)J recombination in 53BP1$^{-/-}$XLF$^{-/-}$ and H2AX$^{-/-}$XLF$^{-/-}$ cells, implying that ATM has H2AX- and 53BP1-independent functions during end joining in XLF$^{-/-}$ cells (Fig. 3) (10). One of these functions might be to promote end resection, as inhibiting ATM kinase activity led to mild hairpin opening defects in XLF-deficient cells and partially prevented end degradation in 53BP1$^{-/-}$XLF$^{-/-}$ and H2AX$^{-/-}$XLF$^{-/-}$ cells (Fig. 3). In this context, ATM phosphorylates substrates directly involved in end processing independent of H2AX or 53BP1, such as MRE11 and CtIP.

Despite the similar functions of H2AX and 53BP1 in end protection, H2AX$^{-/-}$XLF$^{-/-}$ mice are embryonic lethal (10), whereas 53BP1$^{-/-}$XLF$^{-/-}$ mice were born at the expected Mendelian ratio (Fig. S1*A*), implying that the embryonic lethality of H2AX$^{-/-}$XLF$^{-/-}$ mice is not simply due to excessive end resection. Conceivably, the essential function of H2AX in embryonic development could reflect a 53BP1-independent role for H2AX in S/G_2 phase DNA repair as a substrate for ATR or during single-strand annealing (34). Alternatively, 53BP1 deficiency might promote homologous recombination (HR) to support embryonic development in end-joining–deficient 53BP1$^{-/-}$XLF$^{-/-}$ mice, because 53BP1 deficiency rescues the embryonic lethality of BRCA1-deficient mice by promoting HR (35). Another not mutually exclusive possibility is that 53BP1, like ATM, has a prominent role in cell cycle checkpoint control beyond H2AX, allowing 53BP1$^{-/-}$XLF$^{-/-}$ cells to proliferate despite the genomic instability engendered by end-joining defects. The combination of end joining defects and checkpoint defects can often lead to lymphomas as seen with NHEJ/p53 double-deficient mice or ATM$^{-/-}$ mice (1, 36). Consistent with the latter possibility, three of the four 53BP1$^{-/-}$XLF$^{-/-}$ mice we analyzed developed clonal thymic lymphomas (Fig. S10).

Tandem BRCT domains are a characteristic feature of many proteins involved in DNA repair and DNA damage signaling. Surprisingly, we found that the BRCT domain of 53BP1 is not required for end joining in XLF$^{-/-}$ cells. Similarly, the BRCT domain of 53BP1 is dispensable for CSR, another DNA recombination event that requires 53BP1 (26). In contrast, the Tudor domains of 53BP1, and by extension the ability of 53BP1 to form foci at DSBs, are essential for both end-joining and end protection in XLF-deficient cells (Fig. 4 *A* and *B*). Nevertheless, it remains unclear whether the Tudor domain is also required for the checkpoint or tumor suppression functions of 53BP1—a hypothesis that needs to be tested by using in vivo model. A recent study identified the oligomerization domain of 53BP1 is also required for CSR as the Tudor domain (26). In this context, it would be interesting to test whether the oligomerization domain and other domains of 53BP1 are also required for end joining and end protection in XLF-deficient cells in future study. Taken together, our study identifies critical functions for 53BP1 in end-joining, lymphocyte development, and tumor suppression in an XLF-deficient background that are related to, but also distinct from, those of H2AX and ATM.

Experimental Procedures

Mice. XLF$^{-/-}$ (7), 53BP1$^{-/-}$ (32), EμBcl-2 transgenic (31), and Ig Heavy and Light chain knockin mice (29, 30) were described. 53BP1 and EμBcl-2 transgene are closely linked on mouse chromosome 2 (≈1–2 cM from each other based on our breeding). All animal work has been conducted in a pathogen-free facility, and all of the procedures were approved by Animal Care and Use Committee at Columbia University Medical Center.

Lymphocyte Development. Lymphocyte populations at thymus, bone marrow, spleen, and lymph node from 4- to 8-wk-old mice were analyzed by flow cytometry as described before. Approximately 1×10^5 cells were stained by using flourescence-conjugated antibodies as indicated. Flow cytometry was performed on FACSCalibur flow cytometer (BD Bioscience), and data were processed by using Cellquest (BD Bioscience) or FlowJo.

Generation and Analysis of v-abl Transformed Immature B-Cell Lines. Total bone marrow was isolated from various mouse lines with Eμ-Bcl2 transgene and then infected with retrovirus encoding v-abl kinase. Only immature B cells (a mixture of pro- and pre-B cells) could be transformed by v-abl kinase. Cells were maintained in DMEM (GIBCO) with 10% (vol/vol) FBS for 8 wk, before V(D)J recombination substrates were introduced through another round of retrovirus infection. V(D)J recombination with integrated substrates (pMX-INV, pMX-CJ, pMX-SJ) were carried out as before (7, 10, 13). Briefly, v-abl–transformed B cells with stable integration of the substrate were treated with STI571(3 μM; Novartis Pharmaceuticals) and assayed for V(D)J recombination at 0, 2, or 4 d by FACS for GFP expression and by Southern blotting for rearrangement. For Southern blot analysis, DNA from cells contains pMX-CJ or pMX-SJ V(D)J recombination substrates were digested with EcoRV probed with hCD4 probe. DNA from cells containing pMX-INV substrate is digested with either EcoRV or EcoRV+NcoI and probed with hCD4 probe. The hCD4 probe is PCR amplified with primers (5′-GTT CGG ATT GAC TGC CAA CT-3′ and 5′-GAT GCC TAG CCC AAT GAA AA-3′) from pMX-INV plasmid. ATM kinase inhibitor Ku55933 (Tocris) was used at a final concentration of 15 μM.

Construction of Plasmids. pBMN-IRES-GFP was purchased from Addgene, and the GFP is replaced by a truncated humanCD2 fragment to generate pBMN-IRES-hCD2. Full-length mouse XLF or 53BP1 was inserted into the EcoRI and NotI, respectively, of pBMN-IRES-hCD2. To generate 53BP1ΔBRCT (aa 1689–1964 deletion) and 53BP1Tudor-mut (D1518R), proper deletion or point mutation were engineered in pBMN-53BP1-IRES-hCD2 construct and verified by sequencing.

ACKNOWLEDGMENTS. We thank Dr. Richard Baer for his critical comments on the manuscript; Drs. Theresa Swayne, Adam White, and Vundavalli Murty for their generous help on FISH analysis; Drs. Junjie Chen and Klaus Rajewsky for sharing the 53BP1 deficient and Immunoglobulin Heavy/Light Chain knockin mice, respectively; and Erica Chung, James Xie, and Raul Alonso for their technical assistance. This work was supported by National Institutes of Health/National Cancer Institute Grant CA158073 (to S.Z.) and funding was made available by St. Baldrick Foundation and John Driscoll Jr. Children's Medical Award. S.Z. was also supported by a senior fellowship from the Leukemia and Lymphoma Society. K.Y. received support from the Pathobiology and Molecular Medicine graduate program. Z.W. was partially supported by a Summer Undergraduate Research Fellowship from Columbia University.

1. Rooney S, Chaudhuri J, Alt FW (2004) The role of the non-homologous end-joining pathway in lymphocyte development. *Immunol Rev* 200:115–131.
2. Lieber MR (2010) The mechanism of double-strand DNA break repair by the non-homologous DNA end-joining pathway. *Annu Rev Biochem* 79:181–211.
3. Ahnesorg P, Smith P, Jackson SP (2006) XLF interacts with the XRCC4-DNA ligase IV complex to promote DNA nonhomologous end-joining. *Cell* 124:301–313.
4. Buck D, et al. (2006) Cernunnos, a novel nonhomologous end-joining factor, is mutated in human immunodeficiency with microcephaly. *Cell* 124:287–299.
5. Li Y, et al. (2008) Crystal structure of human XLF/Cernunnos reveals unexpected differences from XRCC4 with implications for NHEJ. *EMBO J* 27:290–300.
6. Andres SN, Modesti M, Tsai CJ, Chu G, Junop MS (2007) Crystal structure of human XLF: A twist in nonhomologous DNA end-joining. *Mol Cell* 28:1093–1101.
7. Li G, et al. (2008) Lymphocyte-specific compensation for XLF/cernunnos end-joining functions in V(D)J recombination. *Mol Cell* 31:631–640.
8. Dai Y, et al. (2003) Nonhomologous end joining and V(D)J recombination require an additional factor. *Proc Natl Acad Sci USA* 100:2462–2467.
9. Zha S, Alt FW, Cheng HL, Brush JW, Li G (2007) Defective DNA repair and increased genomic instability in Cernunnos-XLF-deficient murine ES cells. *Proc Natl Acad Sci USA* 104:4518–4523.
10. Zha S, et al. (2011) ATM damage response and XLF repair factor are functionally redundant in joining DNA breaks. *Nature* 469:250–254.
11. Lavin MF (2008) Ataxia-telangiectasia: From a rare disorder to a paradigm for cell signalling and cancer. *Nat Rev Mol Cell Biol* 9:759–769.
12. Bredemeyer AL, et al. (2008) DNA double-strand breaks activate a multi-functional genetic program in developing lymphocytes. *Nature* 456:819–823.
13. Bredemeyer AL, et al. (2006) ATM stabilizes DNA double-strand-break complexes during V(D)J recombination. *Nature* 442:466–470.
14. Barlow C, et al. (1996) Atm-deficient mice: A paradigm of ataxia telangiectasia. *Cell* 86:159–171.
15. Borghesani PR, et al. (2000) Abnormal development of Purkinje cells and lymphocytes in Atm mutant mice. *Proc Natl Acad Sci USA* 97:3336–3341.
16. Helmink BA, et al. (2011) H2AX prevents CtIP-mediated DNA end resection and aberrant repair in G1-phase lymphocytes. *Nature* 469:245–249.
17. Gapud EJ, et al. (2011) Ataxia telangiectasia mutated (Atm) and DNA-PKcs kinases have overlapping activities during chromosomal signal joint formation. *Proc Natl Acad Sci USA* 108:2022–2027.
18. Zha S, et al. (2011) Ataxia telangiectasia-mutated protein and DNA-dependent protein kinase have complementary V(D)J recombination functions. *Proc Natl Acad Sci USA* 108:2028–2033.
19. Callén E, et al. (2009) Essential role for DNA-PKcs in DNA double-strand break repair and apoptosis in ATM-deficient lymphocytes. *Mol Cell* 34:285–297.
20. Difilippantonio S, et al. (2008) 53BP1 facilitates long-range DNA end-joining during V(D)J recombination. *Nature* 456:529–533.
21. Bothmer A, et al. (2010) 53BP1 regulates DNA resection and the choice between classical and alternative end joining during class switch recombination. *J Exp Med* 207:855–865.
22. Celeste A, et al. (2003) Histone H2AX phosphorylation is dispensable for the initial recognition of DNA breaks. *Nat Cell Biol* 5:675–679.
23. Bekker-Jensen S, Mailand N (2010) Assembly and function of DNA double-strand break repair foci in mammalian cells. *DNA Repair (Amst)* 9:1219–1228.
24. Charier G, et al. (2004) The Tudor tandem of 53BP1: A new structural motif involved in DNA and RG-rich peptide binding. *Structure* 12:1551–1562.
25. Joo WS, et al. (2002) Structure of the 53BP1 BRCT region bound to p53 and its comparison to the Brca1 BRCT structure. *Genes Dev* 16:583–593.
26. Bothmer A, et al. (2011) Regulation of DNA end joining, resection, and immunoglobulin class switch recombination by 53BP1. *Mol Cell* 42:319–329.
27. Mak TW, et al. (2000) Brca1 required for T cell lineage development but not TCR loci rearrangement. *Nat Immunol* 1:77–82.
28. Koralov SB, et al. (2008) Dicer ablation affects antibody diversity and cell survival in the B lymphocyte lineage. *Cell* 132:860–874.
29. Pelanda R, Schaal S, Torres RM, Rajewsky K (1996) A prematurely expressed Ig(kappa) transgene, but not V(kappa)J(kappa) gene segment targeted into the Ig(kappa) locus, can rescue B cell development in lambda5-deficient mice. *Immunity* 5:229–239.
30. Lam KP, Kuhn R, Rajewsky K (1997) In vivo ablation of surface immunoglobulin on mature B cells by inducible gene targeting results in rapid cell death. *Cell* 90:1073–1083.
31. Strasser A, et al. (1991) Enforced BCL2 expression in B-lymphoid cells prolongs antibody responses and elicits autoimmune disease. *Proc Natl Acad Sci USA* 88:8661–8665.
32. Ward IM, Minn K, van Deursen J, Chen J (2003) p53 Binding protein 53BP1 is required for DNA damage responses and tumor suppression in mice. *Mol Cell Biol* 23:2556–2563.
33. Pei H, et al. (2011) MMSET regulates histone H4K20 methylation and 53BP1 accumulation at DNA damage sites. *Nature* 470:124–128.
34. Xie A, et al. (2004) Control of sister chromatid recombination by histone H2AX. *Mol Cell* 16:1017–1025.
35. Bunting SF, et al. (2010) 53BP1 inhibits homologous recombination in Brca1-deficient cells by blocking resection of DNA breaks. *Cell* 141:243–254.
36. Zha S, et al. (2010) ATM-deficient thymic lymphoma is associated with aberrant tcrd rearrangement and gene amplification. *J Exp Med* 207:1369–1380.